Does active mantle upwelling help drive plate motions?

Stephen A. Steiner, Clinton P. Conrad *

Department of Earth and Planetary Sciences, Johns Hopkins University, Baltimore, MD 21218, USA

Abstract

Earth's lithospheric plates are driven partly by shear tractions exerted on their base by viscous coupling to convective mantle flow. While downwelling flow associated with descent of subducted lithosphere has been well established as a driver of plate motions, the plate-driving role of upwelling flow is more controversial. We used a numerical mantle flow model to predict present-day plate motions driven by various combinations of upwelling and downwelling flow. We obtain a good fit to observed plate motions using flow driven only by downgoing mantle slabs, whose densities can be inferred either from the tectonic history of subduction or from positive velocity anomalies extracted from mantle tomography. Introducing upwelling flow (driven by negative density anomalies inferred from slow seismic velocity anomalies) to this slab-driven flow field generally degrades the fit to plate motions, and an acceptable fit that includes active upwelling requires amplitudes of mantle density heterogeneity that are at the low end of the accepted range (tomography to density conversion factor = 0.05 g cm^{-3} km^{-1} s). Because such small amplitudes lead to a deficit of slab material in the mantle, we infer that downwelling flow is a more significant driver of plate motions than upwelling flow. This conclusion can be reconciled with the presence of low-velocity anomalies in the lower mantle if upwelling flow does not couple effectively to plate motions, or if these low-velocity anomalies represent chemical differentiation of the lower mantle and thus do not drive upwelling flow.
© 2007 Elsevier B.V. All rights reserved.

Keywords: Convective upwelling; Plate driving forces; Plate tectonics; Seismic tomography; Superplume; Mantle slabs; Mantle convection; Slab pull; Plate–mantle coupling

1. Introduction

The motions of Earth's lithospheric plates are thought to represent the surface expression of convective flow in the Earth's viscous mantle (e.g., Turcotte and Oxburgh, 1967). Studies of the force balance on plates (e.g., Forsyth and Uyeda, 1975; Richter and McKenzie, 1978; Lithgow-Bertelloni and Richards, 1998; Becker and O'Connell, 2001; Conrad and Lithgow-Bertelloni, 2002,

2004) indicate that tectonic plate motions are driven primarily by subducting slabs and the downwelling flow associated with their descent. In fact, the basic patterns of observed plate motions have been predicted for the present-day (e.g., Becker and O'Connell, 2001; Conrad and Lithgow-Bertelloni, 2002) and throughout the Cenozoic (Conrad and Lithgow-Bertelloni, 2004) using a model in which lower mantle slabs drive downwelling flow that exerts tractions on the base of plates (slab suction) and upper mantle slabs exert a "slab pull" force directly on subducting plates (e.g., Elsasser, 1969). Because the upper boundary layer for mantle convection (the lithosphere) dominates convective flow for an internally heated system such as the mantle (e.g., Davies,

* Corresponding author. Tel.: +1 410 516 3922;
fax: +1 410 516 7933.

E-mail address: conrad@jhu.edu (C.P. Conrad).

1988), it is not surprising that subduction of the lithosphere generates the primary driving forces for plates.

There has been some controversy, however, over the convective source of the basal shear tractions that drive plate motions. Conrad and Lithgow-Bertelloni (2002) describe the slab suction force as the integrated shear tractions that downwelling flow exerts on the base of each plate. They find that slab suction accounts for approximately 40% of the driving forces on plates. Because slabs are typically located beneath subduction zones, slab descent typically generates a pattern of flow that drives plates toward subduction zones. Other patterns of mantle flow, however, are possible. For example, Lithgow-Bertelloni and Silver (1996) have suggested that viscous flow driven by warm upwellings could also generate mantle flow that exerts basal shear tractions on plates. Such upwelling-induced tractions have not been considered as a potential driver of plate motions by authors that use subduction history to infer mantle density heterogeneity (e.g., Lithgow-Bertelloni and Richards, 1998; Conrad and Lithgow-Bertelloni, 2002, 2004). However, we expect upwelling flow in the mantle associated with plumes ascending from the lower boundary layer. Such plumes are likely to excite only small-scale flow because plume conduits are typically only ∼100 km wide or less (e.g., Richards et al., 1989). Thus, the influence of rising plumes is probably not significant for plate-scale flow. Potentially more important, however, are large, low-velocity anomalies that are observed beneath Africa and the South Pacific (Dziewonski and Woodhouse, 1987; Su et al., 1994; Li and Romanowicz, 1996; Grand et al., 1997; Ritsema et al., 1999). If these low-velocity anomalies have a thermal origin, then they should represent hot rising mantle that is 1000s of km across. There is evidence of a thermal origin for the African anomaly in particular, because radial patterns of seismic anisotropy surrounding southern Africa suggest the presence of active upwelling (Behn et al., 2004). Similarly, dynamic topography produced by active upwelling can explain the unusually high present-day topography of southern Africa (Lithgow-Bertelloni and Silver, 1998), as well as the geologic history of this uplift (Conrad and Gurnis, 2003). If this upwelling mantle flow is present, it should contribute to the basal shear tractions on plates, and thus should be added to the balance of forces on plates.

Several studies, however, have suggested a chemical origin for these low-velocity anomalies based on seismological and geochemical evidence (e.g., Kellogg et al., 1999; van der Hilst and Karason, 1999; Masters et al., 2002). In this case, these low-velocity anomalies may represent compositionally distinct "piles" (e.g., Davaille, 1999; McNamara and Zhong, 2004, 2005) that sit in the lower mantle but deform in response to mantle-scale flow. This interpretation would explain several attributes of these anomalies that cannot be explained by thermal effects alone (e.g., van der Hilst and Karason, 1999; Masters et al., 2002; Ni et al., 2002), but would not produce active upwelling flow.

In this study, we use a tomographic model of mantle shear velocity anomalies to construct models for mantle density heterogeneity that are dominated by either downwelling slabs (positive shear velocity anomalies), upwelling "superplumes" (negative shear velocity anomalies), or a combination of both. We then calculate the viscous mantle flow driven by these density heterogeneity models, and determine the shear stresses that this flow exerts on the base of the plates. By balancing the forces on each plate, we can predict the plate motions that each flow pattern would produce. By comparing these predicted plate motions to observed present-day plate motions, we attempt to determine whether active upwelling flow contributes to the forces that drive plate motions.

2. Mantle density heterogeneity and plate motions

Ultimately, surface plate motions are driven by the action of gravity on the mantle's interior density heterogeneity structure. Several studies have used different models for this density heterogeneity structure to constrain various aspects of mantle flow. For example, Becker and O'Connell (2001) found that a model of density heterogeneity based on the tectonically constrained history of subduction (referred to as the "slab model" here) (Ricard et al., 1993; Lithgow-Bertelloni and Richards, 1998; Steinberger, 2000) produces a better fit to observed plate motions than does a model of density heterogeneity based on any one of several different seismic tomography models. Conrad and Lithgow-Bertelloni (2002) were able to produce an even better fit to plate motions (Fig. 1) by ignoring the viscous flow generated by the descent of upper mantle slabs and instead imposing the upper mantle slab weight as an edge force on the subducting boundary of subducting plates. In particular, the upper mantle slabs must exert a strong pull force on subducting plates in order to explain the observation that subducting plates move three to four times faster than overriding plates.

Tomographic models of mantle density heterogeneity use large datasets of seismic travel times to invert for a three-dimensional model of seismic wave speed (e.g., Grand et al., 1997; Ritsema et al., 1999, 2004). Because the seismic wave speed increases with density,

(A)   Predicted Plate Motions-Slab Model   **(B)   Observed Plate Motions**

Velocity/Average Velocity

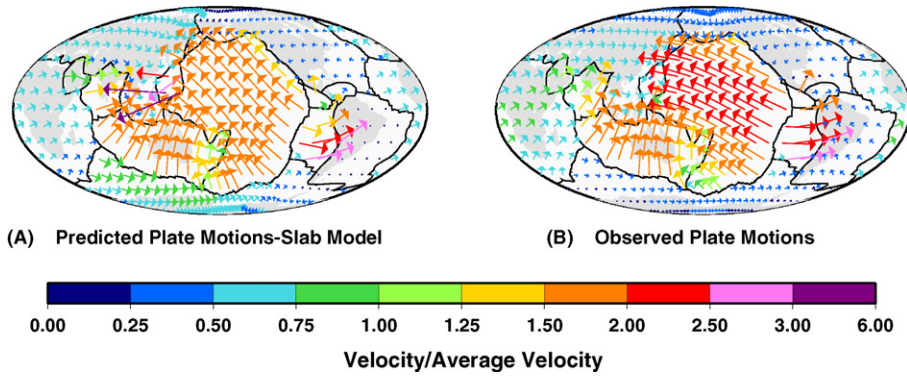0.00   0.25   0.50   0.75   1.00   1.25   1.50   2.00   2.50   3.00   6.00

Fig. 1. Present-day plate motions (A) predicted using the method of Conrad and Lithgow-Bertelloni (2002, 2004), which combines slab pull from upper mantle slabs and slab suction from lower mantle slabs (slab locations and densities inferred from the slab model of Lithgow-Bertelloni and Richards (1998)) and (B) observed using rotation poles defined by the NUVEL-1A (no net rotation) model (DeMets et al., 1994). The average misfit between these two fields is 0.39, which we use as a reference against which to compare plate motions predicted by other models of mantle density heterogeneity.

217.5 km

1522.5 km

652.5 km

1957.5 km

1087.5 km

2392.5 km

V_s Anomaly (%)

-0.8   -0.6   -0.4   -0.2   -0.1   0.0   0.1   0.2   0.4   0.6   0.8
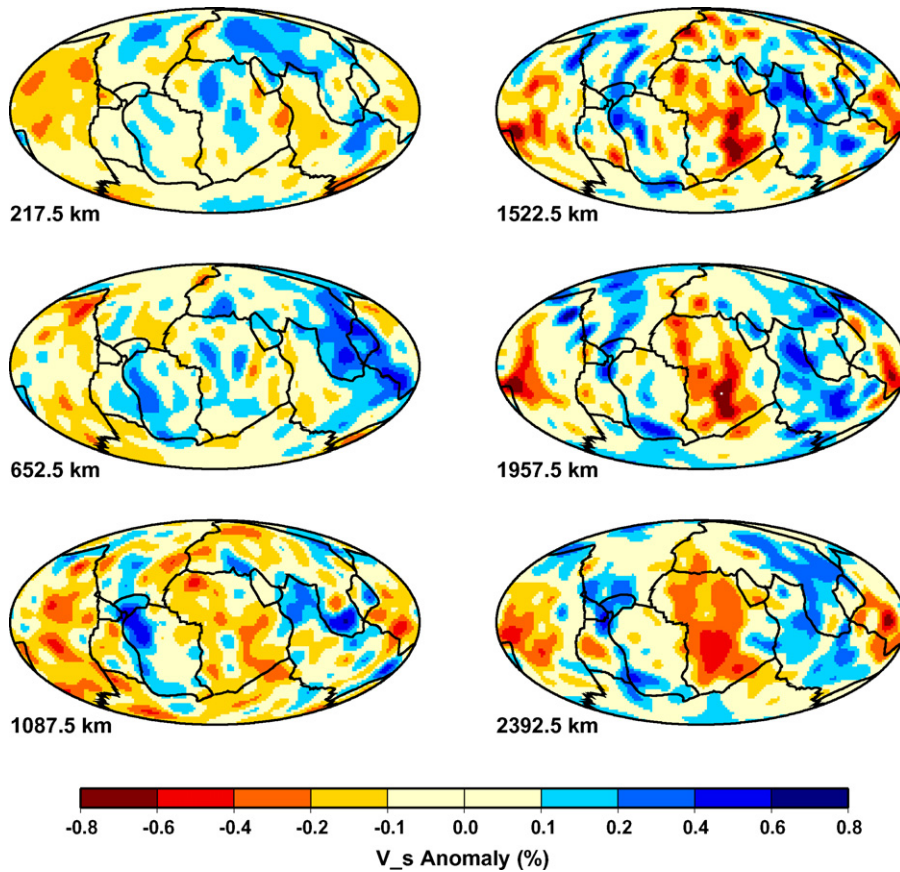
Fig. 2. Tomography model S20RTSb (Ritsema et al., 2004), given as a fractional anomaly in shear wave speed, for six mantle depths. Blue regions exhibit faster than average seismic velocities (positive anomalies), and are generally thought to correspond to dense subducted slabs. Velocities in red regions are slower than average (negative anomalies), and may or may not correspond to hot, low-density, upwellings. (For interpretation of the references to colour in this figure legend, the reader is referred to the web version of the article.)

fast seismic velocity anomalies are generally interpreted to be cold, dense, subducted lithosphere (e.g., Becker and Boschi, 2002). Because seismic tomography should detect the actual distribution of anomalies associated with slab subduction, we would expect flow models driven by tomographically inferred density heterogeneity to better predict plate motions than flow models driven by the assumed distribution in the slab model. The fact that they do not (Becker and O'Connell, 2001), can be explained in one of two ways. First, it is possible that poor data coverage leaves some areas of the mantle poorly sampled by tomography, thus preventing a full accounting of the mantle's slab inventory by tomography. Alternatively, we note that when density heterogeneity is inferred from tomography models in a straightforward way, the slow-velocity anomalies present in tomography produce positive density anomalies (Fig. 2) that are not present in the slab model. If low-velocity seismic anomalies represent compositional heterogeneity, rather than regions of hot mantle as assumed by Becker and O'Connell (2001), then they might not drive active upwelling flow. The fact that thermal upwelling flow is included in Becker and O'Connell's (2001) tomographically driven flow models may explain why plate motions driven by these flow models predict observed plate motions more poorly than flow models driven by downwelling slabs alone. In this study, we examine the role of upwelling mantle flow for driving plate motions by separating the positive and negative velocity anomalies in a tomographic model, driving plate motions by assuming a thermal origin for each, and then comparing the predicted velocity fields to observed plate motions. In doing so, we find that the presence of active upwelling associated with slow seismic velocity anomalies generally degrades the fit to plate motions.

3. Predicting plate motions

We use a spectral method to compute instantaneous mantle flow (Hagar and O'Connell, 1979; Hager and O'Connell, 1981) driven by different models of mantle density heterogeneity. To compute the plate motions driven by this flow, we follow the method of Lithgow-Bertelloni and Richards (1998). In doing so, we calculate plate-driving torques for each of 13 plates (we use the boundaries of Lithgow-Bertelloni and Richards' (1998) 12 plate model, and separate the Indian and Australian plates using the boundary defined by Bird (2003)) by integrating the shear tractions that viscous flow exerts on the base of each plate. Resisting forces are determined by imposing a unit velocity for each plate in each Cartesian direction, and measuring the resisting tractions

that viscous drag exerts on each plate. By balancing the driving and resisting torques for each plate, we invert for the set of plate motions that will allow the net force on each plate to be zero. For some models, we include the slab pull force in the force balance because Conrad and Lithgow-Bertelloni (2002) showed that it is an important driver of plate motions. In these cases, we remove density heterogeneity in the upper mantle (for densities inferred from tomography, we only remove the positive velocity anomalies because negative velocity anomalies do not correspond to slabs) and instead add an edge force equal to the weight of upper mantle slabs to subducting plate boundaries, following the method of Conrad and Lithgow-Bertelloni (2002, 2004). Using this combination of slab suction from lower mantle slabs (locations and densities inferred from the "slab model") and slab pull from upper mantle slabs, we reproduce the results of Conrad and Lithgow-Bertelloni (2002, 2004) for the present-day (Fig. 1A).

We quantitatively compare different predictions of plate motions to the NUVEL-1A (DeMets et al., 1994) observed plate motions (Fig. 1B), using the misfit function described by Conrad et al. (2004). This misfit function uses the area-weighted average magnitude (on a $1° \times 1°$ grid) of the difference between predicted and observed plate motion vectors, in a no-net rotation reference frame. We first scale the magnitude of predicted plate motions so that the average speed of plates is equal to that of observed plate motions. This is permissible (e.g., Lithgow-Bertelloni and Richards, 1998; Conrad and Lithgow-Bertelloni, 2002) because plate speeds are inversely related to the absolute mantle viscosity, which is uncertain by at least a factor of 3. The misfit function is slightly sensitive to the radial viscosity structure (Conrad and Lithgow-Bertelloni, 2004); here we use a radially symmetric viscosity structure that provides a best fit to the geoid (Lithgow-Bertelloni and Richards, 1998). This structure includes a lower mantle layer below 670 km and a lithosphere above 130 km that are 50 and 10 times the upper mantle viscosity, respectively.

The misfit function is primarily sensitive to differences between predicted and observed plate motions, as well as spatial variations in the magnitude of plate motions. To characterize this sensitivity, we have plotted the misfit function for various discrepancies between predicted and observed plate motions (Fig. 3). First, we consider a case in which predicted plate velocity vectors have the correct magnitude, but are oriented in a direction that differs from the observed direction by an angle θ. The misfit in this case is given by the expression $(2Av/v_{avg}) \sin(\theta/2)$, where v is the average plate speed over a given areal fraction A of the earth's sur-
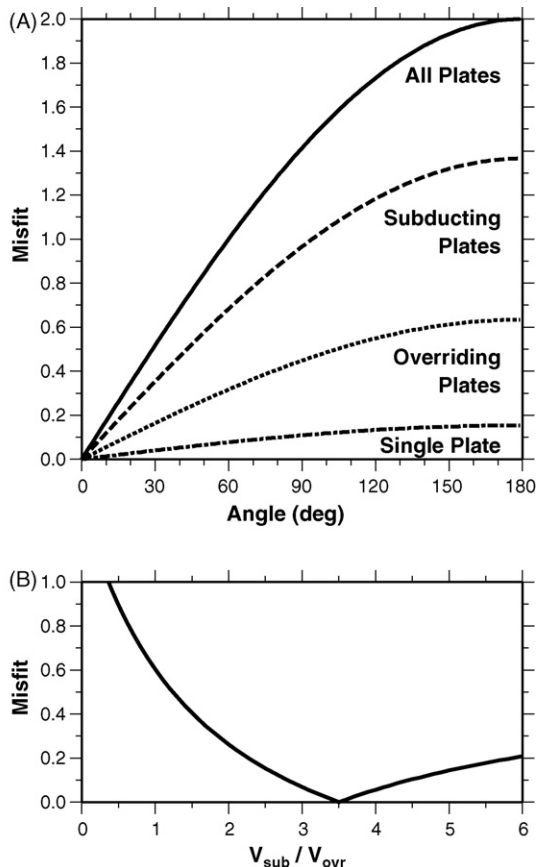
Fig. 3. The misfit function for hypothetical discrepancies between predicted and observed plate motions. (A) The misfit if all plates move with the correct observed speed, but either all plates (solid line), the subducting plates (dashed line), the overriding plates (dotted line), or a single "average" plate (dash-dot line) move in a direction that is an angle θ away from the observed direction. (B) The misfit if the ratio of subducting to non-subducting plate speeds (V_{sub}/V_{ovr}) differs from the observed value of 3.5.

face, and v_{avg} is the global average plate speed. If the misfit angle is constant over the entire surface of the earth, the misfit increases from 0 to 2 as the θ increases from 0° to 180° (Fig. 3A, solid line). For small angles (less than ~60°), the misfit increase is approximately linear with θ with a slope of 0.017 per degree. If the misfit is confined to subducting plates only (the Pacific, Indian, Australian, Nazca, Cocos, and Philippine plates, which cover 38.1% of the earth's surface and move an average of 3.5 times faster than the overriding plates), the net misfit will be smaller (Fig. 3A, dotted line). A further decrease is expected if the misfit is confined to the overriding plates only (Fig. 3A, dotted line), because these plates move more slowly despite covering a larger area. Finally, if only a single plate of average velocity and average area (1/13th of the global area, which is

slightly smaller than the South American plate), moves in a direction θ away from the observed direction, the calculated misfit will be 1/13th of that for the entire globe (Fig. 3A, dash-dot line).

The misfit function is also sensitive to the relative amplitudes of plate speeds. For example, a nonzero misfit results if all plates are moving in the correct direction, but the ratio of subducting to overriding plate speeds differs from the observed ratio of 3.5 (Fig. 3B). Of course actual misfit estimates from model predictions are the combined result of discrepancies in both plate speed and direction, and thus are generally larger than the misfits shown in Fig. 3. However, these end-member examples of the dependence of misfit on θ or V_{sub}/V_{ovr} are useful for calibrating changes in misfits obtained from model predictions against hypothetical changes in the predicted plate velocity field. For example, if the direction of a single plate of average area and speed rotates by 90° to match the observed plate motion, the misfit estimate will decrease by 0.11 (Fig. 3A, dash-dot line). This corresponds to the direction of all plates, subducting plates, or overriding plates improving by 6.3°, 9.2°, or 20°, respectively (Fig. 3A). Alternatively a decrease in misfit of 0.11 corresponds to a change in the V_{sub}/V_{ovr} ratio from 2.7 to 4.6 to the observed present-day ratio of 3.5 (Fig. 3B). All of these scenarios represent a significant improvement in the fit to plate motions. For comparison, Conrad et al. (2004) found that the introduction of slab pull from upper mantle slabs improved the misfit function by about 0.11 compared to slab suction operating alone.

We use the S20RTSb tomography model (Ritsema et al., 2004) to infer mantle density heterogeneity. In order to convert shear velocity anomalies given by this tomography model (Fig. 2) into density anomalies for driving viscous mantle flow, we employ a constant tomography conversion factor (TCF) throughout the mantle. Because our misfit function (described above) is insensitive to the absolute magnitude of plate speeds, our choice of a TCF is not important for predictions of plate motions driven only by flow from tomographically inferred density heterogeneity. However, if slab pull is also included in the balance of forces on plates, then the choice of TCF becomes important because it controls the relative importance of tomographically inferred mantle densities and the slab pull force, which is based on the tectonically constrained weight of upper mantle slabs. In these cases, we examine a range of values for the TCF approximately centered around $0.15\,\text{g cm}^{-3}\,\text{km}^{-1}\,$s (corresponding to $d\ln(p)/d\ln(v_s)$ 0.2 using the terminology of Karato and Karki (2001)), which has been used by previous authors (e.g., Thoraval and Richards, 1997; Becker et al., 2003; Behn et al., 2004) and is within the range

of extreme estimates for TCF that vary from ∼0.05 to ∼0.4 g cm^{-3} km^{-1} s, based on geodynamic (e.g., Gurnis et al., 2002) and laboratory (e.g., Karato and Karki, 2001) constraints. Although we examine a range of TCF, we do not investigate the possibility that TCF may vary with depth (Karato and Karki, 2001).

4. Results: plate motions driven by mantle density heterogeneity

We test various combinations of density models to determine if upwelling flow improves the fit to plate motions. To do this, we separate the negative and positive velocity anomaly components of the S20RTSb tomography model (Ritsema et al., 2004) and use the densities inferred from these anomalies to drive plate motions. By determining how the fit to plate motions changes for different contributions of positive or negative density anomalies, we can determine the relative importance of each for driving plate motions.

4.1. Slab model

We start with the slab model, which is constructed using the history of subduction since the mid-Mesozoic by dropping slabs into the mantle beneath converging plate boundaries (Lithgow-Bertelloni and Richards, 1998). This model contains only positive density anomalies and has been used by several authors to successfully predict plate motions. When the slab model is used to drive mantle flow, the basic direction of motion is predicted for most plates (e.g., Lithgow-Bertelloni and Richards, 1998), yielding a misfit of 0.65 (Fig. 4, solid black line). Conrad and Lithgow-Bertelloni (2002) showed that allowing upper mantle slabs to drive plate motions via slab pull improves the prediction of relative plate speeds. The introduction of slab pull (Fig. 1A) improves the misfit to 0.39 (Fig. 4, dashed black line). Conrad et al. (2004) obtained a misfit of 0.51 for this same model, but used a different set of observed plate motions (based on poles of rotation from Gordon and Jurdy (1986) and O'Connor and Le Roex (1992) rather than the 13 plate NUVEL-1A model (DeMets et al., 1994)) to calculate their misfit. When upper mantle slab pull is added to the slab model (Fig. 1A), plates with attached slabs (subducting plates) move an average of $V_{sub}/V_{ovr} = 3.8$ times faster than plates without attached slabs (overriding plates) because subducting plates have the added slab pull force acting on them (Fig. 5, dashed black line). This ratio is about 3.5 for the NUVEL-1A (DeMets et al., 1994) observed plate motions (Fig. 5, solid black line). Thus we confirm Conrad and Lithgow-
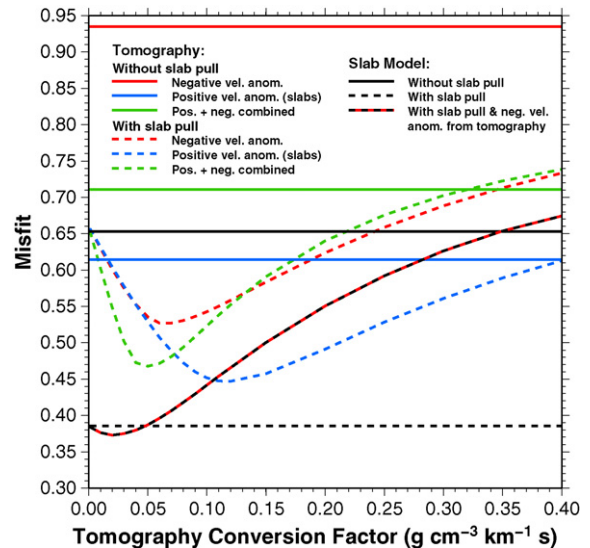

Fig. 4. Misfit between predicted and observed plate motions as a function of tomography conversion factor (TCF) for various models of mantle density heterogeneity. Black lines show misfits for the slab model (Lithgow-Bertelloni and Richards, 1998) both with (dashed) and without (solid) slab pull. Blue lines (or red lines) show misfits for density models in which positive (or negative) velocity anomalies have been isolated from the S20RTSb tomography model (Ritsema et al., 2004) and used to create a model for mantle density heterogeneity that includes only positive (or negative) density anomalies associated with downgoing slabs (or mantle upwelling). Green lines correspond to the combination of positive and negative anomalies, and thus represent a straightforward translation between seismic velocity anomaly and density heterogeneity. The red-black dashed line shows the misfit for a density heterogeneity model composed of positive density anomalies associated with the slab model and negative velocity anomalies extracted from the S20RTSb tomography model. In all cases, dashed and solid lines indicate the presence and absence of slab pull, respectively. (For interpretation of the references to colour in this figure legend, the reader is referred to the web version of the article.)

Bertelloni's (2002, 2004) result that the slab model separated into upper mantle slab pull and lower mantle slab suction does a good job of predicting plate motions.

4.2. Positive velocity anomalies from tomography

To test whether slabs imaged from tomography also provide a good prediction of plate motions, we extract the positive velocity anomalies (primarily corresponding to subducted slabs) from the S20RTSb tomography model (Ritsema et al., 2004). We find that using only the positive velocity anomalies to drive plate motions (Fig. 6A) produces a misfit of 0.61 (Fig. 4, solid blue line). The misfit, as well as the ratio of V_{sub}/V_{ovr} (1.80), remain constant for changing TCF if we do not consider slab pull. Thus we find that in the absence of slab pull, plate motions driven by "slabs" inferred from tomogra-
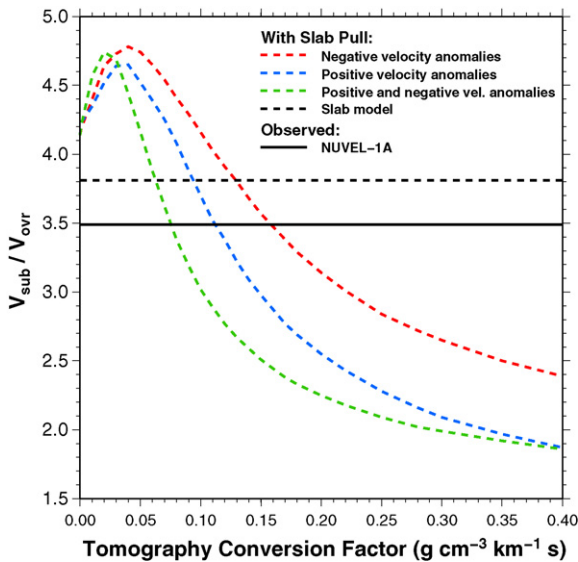
Fig. 5. The ratio of the area-weighted average speed of subducting plates (V_{sub}) compared to that of overriding plates (V_{ovr}), as a function of tomography conversion factor (TCF), for plate motions driven by densities inferred from negative (red), positive (blue), and combined negative and positive (green) velocity anomalies. Also shown is this ratio for the slab model (dashed black line) and observed plate velocities (solid black line) for the NUVEL-1A (DeMets et al., 1994) plate velocity model. Subducting plates include the Pacific, Indian, Australian, Nazca, Cocos, and Philippine plates; others are considered overriding. (For interpretation of the references to colour in this figure legend, the reader is referred to the web version of the article.)

phy (positive velocity anomalies) predict observed plate motions slightly better than those driven by the slab model (misfit 0.65). This suggests that the mantle inventory of slabs is as well represented by tomography as it is by the slab model.

If we include the slab pull force, plate motions predicted by positive velocity anomalies from tomography (Fig. 6B) improves the misfit to a best-fitting value of 0.44 for a TCF of 0.12 g cm^{-3} km^{-1} s (Fig. 4, blue dashed line). This result is nearly as good as we found for the slab model with upper mantle slab pull (0.39, Fig. 1A, four dashed black line). Comparing Figs. 1A and 6B, we see that both models for slab locations offer similar predictions of plate motions, and that both predictions closely resemble observed plate motions (Fig. 1B). In both predicted models, however, the Pacific plate moves in a more northerly direction than is observed due to strong slab pull toward the subduction zones in the Northeast Pacific (e.g., Conrad et al., 2004). The Eurasian plate is predicted to move toward Southeast Asia more strongly than is observed, possibly because of strong slab suction from the plethora of subducted material in this region. Both models appear to produce good

predictions for the Indian, Australian, Nazca, African and North American plates.

The ratio V_{sub}/V_{ovr} decreases with increasing TCF (Fig. 5, blue dashed line) because increasing the density of lower mantle slab material increases the importance of slab suction, which drives subducting and overriding plates symmetrically toward subduction zones. The value of V_{sub}/V_{ovr} is comparable to the observed value of 3.5 for a TCF of 0.12 g cm^{-3} km^{-1} s (Fig. 5), which also provides the best fit to plate motions (Fig. 4). The ratio of V_{sub}/V_{ovr} decreases in both directions away from a maximum at about 0.04 g cm^{-3} km^{-1} s due to a reversal in the direction of overriding plate motions (from trenchward to landward) as the importance of slab pull increases (Conrad and Lithgow-Bertelloni, 2002). Thus, both the misfit and the V_{sub}/V_{ovr} ratio are well predicted by both the slab model and tomographically inferred slab locations (positive velocity anomalies); both models for mantle density heterogeneity do a good job of predicting plate motions through the combination of slab pull and subduction-induced downwelling.

4.3. Negative velocity anomalies from tomography

To test the potential influence of upwelling flow for driving plate motions, we extract the negative velocity anomalies from the tomography model S20RTSb (Ritsema et al., 2004). If we assume that these have a thermal origin, then they should correspond to negative density anomalies and generate upwelling flow. The plate motions predicted to result from this flow (Fig. 6C) produce a misfit of 0.93 (Fig. 4, solid red line). The relatively poor prediction of plate motions for this model is not surprising because negative velocity anomalies contain no information about slabs, which we know to be important for driving plate motions. Yet, upwelling flow does drive several plates in directions similar to those that are observed. For example, several plates are pushed away from the upwelling beneath the south Pacific. This flow tends to drive the Pacific and Nazca plates rapidly apart, as is observed, but it also drives the Australian plate toward the west, which is not. Upwelling flow beneath Africa tends to push the African plate northward, the Indian plate northeastward, and Eurasia southeastward (Fig. 6C), all of which approximately follow observed trends (Fig. 1B).

If we add the slab pull forces from upper mantle slabs to basal tractions driven by upwelling flow, predicted plate motions (Fig. 6D) provide a better match to observed plate motions, and the misfit improves to 0.53 (Fig. 4, red dashed line) for TCF ~0.08 g cm^{-3} km^{-1} s. The ratio of V_{sub}/V_{ovr} for this value of TCF is nearly 4.5,

(A) Positive Anomalies Only-No Slab Pull

(B) Positive Anomalies Only-With Slab Pull

(C) Negative Anomalies Only-No Slab Pull

(D) Negative Anomalies Only-With Slab Pull

(E) Combined Tomography-No Slab Pull

(F) Combined Tomography-With Slab Pull
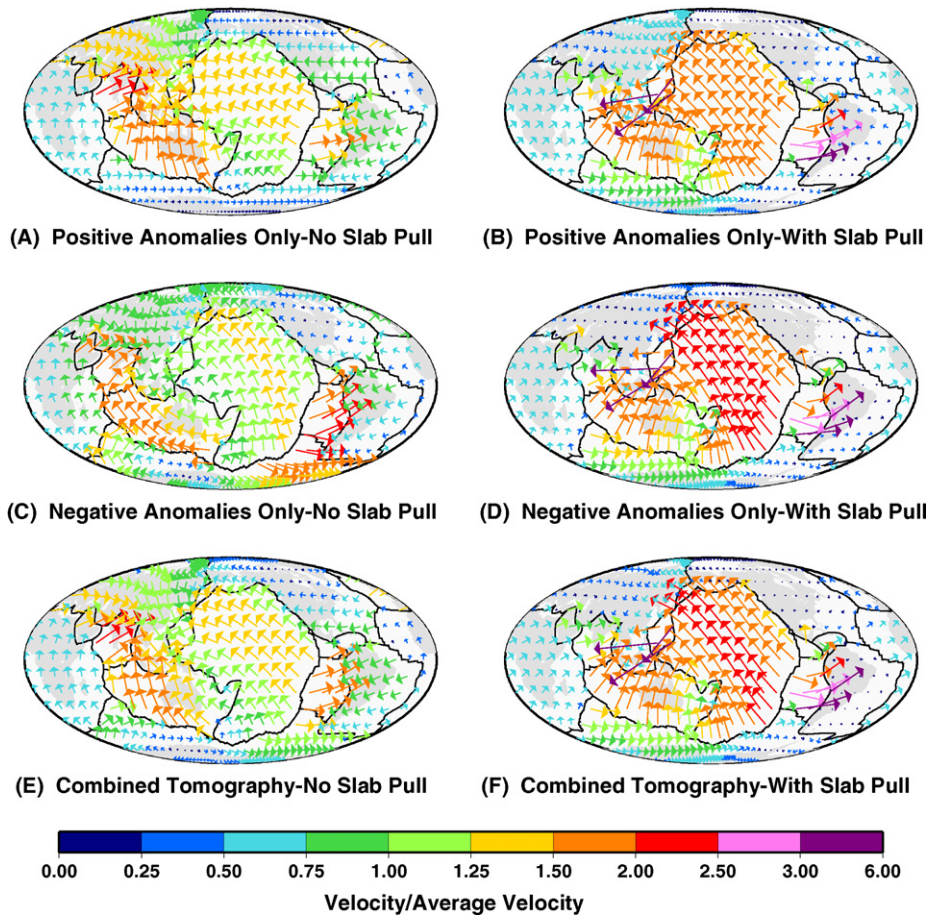
Velocity/Average Velocity

Fig. 6. Plate motions predicted from mantle flow driven by (A and B) positive density anomalies inferred from positive seismic velocity anomalies, (C and D) negative density anomalies inferred from negative seismic velocity anomalies, and (E and F) the combination of positive and negative anomalies. Slab pull from upper mantle slabs is not included in parts A, C, and E, but is included in parts B, D, and F. When slab pull is included, we show the prediction of plate motions that best fits observed plate motions (corresponding to the minima of the relevant curves in Fig. 4). The associated tomography conversion factors are 0.12, 0.08, and 0.05 g cm^{-3} km^{-1} s for parts B, D, and F, respectively.

which is larger than the observed value of 3.5 (Fig. 5). The set of predicted plate motions for the best-fitting TCF (Fig. 6D) compares favorably with both observed plate motions (Fig. 1B), as well as slab driven flow inferred from the slab model (Fig. 1A) or tomography (Fig. 6B). This demonstrates that the slab pull force exerts a significant influence on plate motions, but also that both upwelling and downwelling flow tend to drive most plates in similar directions. However, the fact that a smaller value of TCF is indicated for upwelling flow suggests that upwelling flow must be deemphasized compared to the slab pull force in order to achieve the best fit to plate motions. This confirms the conclusion of previous researchers (e.g., Becker and O'Connell, 2001) that the slab signal, either imaged by tomography or predicted by geodynamic models, is an essential driver of plate motions.

4.4. Combined negative and positive velocity anomalies from tomography

It is perhaps more reasonable to examine the effect of upwelling flow when it is combined with slab-induced downwelling flow, which we have already shown to be an important driver of plate motions. To test this, we combine negative velocity anomalies (upwellings) with the positive velocity anomalies (slabs) and predict plate motions, first without considering slab pull. The result (Fig. 6E) is a combination of the patterns we found for upwelling (Fig. 6A) and downwelling (Fig. 6C) flow, and produces a misfit of 0.71 (Fig. 4, solid green line). Adding slab pull (Fig. 6F) improves the misfit to 0.47 (Fig. 4, green dashed line), but only for small values of TCF near 0.05 g cm^{-3} km^{-1} s. The resulting plate motions (Fig. 6F) yield a good fit to observed plate

motions (Fig. 1B) for a TCF of 0.05 g cm^{-3} km^{-1} s, and produce a ratio V_{sub}/V_{ovr} of about 4, which is slightly larger than is observed (Fig. 5). The best-fit value of TCF = 0.05 g cm^{-3} km^{-1} s is at the very low end of the range of TCF values generally considered (e.g., Gurnis et al., 2002; Karato and Karki, 2001). Such a low value is required for the combination of upwelling and downwelling flow because both flow patterns tend to drive similar patterns of plate motions. Thus, the combined effect of both flows will generate tractions that overwhelm the slab pull force unless their effect is diminished by a small value of TCF. Thus, the inclusion of upwelling flow produced by low-velocity anomalies tends to degrade the fit to plate motions and requires a significantly smaller value of TCF compared to positive velocity anomalies alone.

4.5. Slab model plus negative velocity anomalies from tomography

Observed plate motions are best fit by slab pull and downwelling flow driven by positive density anomalies inferred from the slab model (Fig. 4, dashed black line). Thus, the slab model provides a good reference model against which to test density heterogeneity models that also include negative density anomalies. We added negative density anomalies inferred from negative velocity anomalies (from the S20RTSb tomography model, Ritsema et al. (2004)) to the positive density anomalies of the slab model, and included slab pull from upper mantle slabs. We varied the TCF to adjust the amplitude of active upwelling relative to slab-driven flow. For small TCF < 0.05 g cm^{-3} km^{-1} s, the misfit is essentially unchanged compared to the slab model alone (Fig. 4, red and black line). When upwelling flow is further amplified by increasing the TCF to values larger than 0.05 g cm^{-3} km^{-1} s, the misfit to observed plate motions steadily increases. This suggests that active upwelling provides at most only a minor contribution to the forces that drive plate motions.

5. Discussion

Our finding that active upwelling tends to degrade the fit to plate motions does not necessarily indicate that active upwelling is not present in the mantle. In fact, the tractions that upwelling flow exerts on plates tend to drive the plates in directions that are similar to those that downwelling flow tends to produce (compare Fig. 6A and C). Thus, a reasonably good fit to plate motions can be obtained by either upwelling flow (Fig. 6B), downwelling flow (Fig. 6D), or the combination of both (Fig. 6F), if slab pull is included as a boundary force on subducting plates. However, a good fit to plate motions is only obtained if the magnitude of flow-driven tractions are such that they properly balance the amplitude of the slab pull force, which is well constrained by recent subduction history (Lithgow-Bertelloni and Richards, 1998; Conrad and Lithgow-Bertelloni, 2004). For the combination of upwelling and downwelling flow (driven by straightforward conversion of tomographic velocity anomalies to density anomalies throughout the mantle), this balance requires the magnitude of tomographically inferred mantle density heterogeneity to be on the very low end (TCF = 0.05 g cm^{-3} km^{-1} s) of the range constrained by laboratory and geodynamic studies (TCF between 0.05 and 0.4 g cm^{-3} km^{-1} s).

Alternatively, a good fit to plate motions can be obtained if a different conversion between velocity and density (TCF) applies for positive and negative velocity anomalies. Because positive density anomalies associated with slabs are clearly apparent in tomographic models (e.g., van der Hilst et al., 1997) while the presence of negative density anomalies in the mantle is debated (e.g., Kellogg et al., 1999), one obvious choice is to use a value of TCF in the middle of a reasonable range (best fit for TCF $\sim$ 0.12 g cm^{-3} km^{-1} s) for the positive velocity anomalies and a much smaller (or negligible) value for upwellings. In this case, plate motions driven by the combination of slab pull and basal shear tractions associated with slab-driven downwelling fit observed plate motions well (Fig. 6B) while maintaining a conversion factor between seismic velocity anomaly and density that is within the center of the reasonable range.

Thus, we can obtain a good fit to plate motions either with or without active upwelling flow from the lower mantle. However, we find that mantle flow dominated by slab-induced downwelling flow and the passive response of seismically slow regions of the mantle beneath Africa and the South Pacific provides the most likely explanation for observed plate motions because a more reasonable value of the conversion between seismic velocity anomalies and density applies. However, because plate motions respond to the net mantle traction beneath each plate, oppositely directed tractions acting on the same plate will not contribute to plate motions. Some of the major upwellings occur beneath the center of the African and Pacific plates (Fig. 2), so the radially directed tractions produced by these upwellings may not act as efficient drivers of plate motions. As a result, combinations of observations that are sensitive to the local flow field, such as seismic anisotropy (e.g., Behn et al., 2004), the intraplate lithospheric stress field (e.g.,

Steinberger et al., 2001; Lithgow-Bertelloni and Guynn, 2004), or dynamic topography (e.g., Lithgow-Bertelloni and Silver, 1998; Conrad and Gurnis, 2003) may be more sensitive indicators of the presence of upwelling-induced mantle flow.

Our results do not eliminate the possibility that the seismically slow regions of the mantle could represent active upwelling flow, but that this upwelling flow does not drive plate motions as effectively as does downwelling flow. This would be the case if plate-driving tractions generated by active upwelling occur in regions of poor plate-mantle coupling. These tractions will be largest some distance away from the location of upwelling as the flow spreads out radially beneath the lithosphere (Behn et al., 2004). If the viscosity of the sub-lithospheric mantle is diminished in these regions by the hot temperatures associated with the upwelling itself, the plate-driving potential of the upwelling will be diminished. In addition, because African and South Pacific upwellings rise beneath the center of plates, the largest plate-driving tractions generated by upwelling will occur away from the mid-plate regions and closer to plate boundaries. Conrad and Lithgow-Bertelloni (2006) showed that plate-driving tractions are diminished in regions of thin lithosphere, so the positioning of the largest tractions beneath the thin lithosphere of ridges (circum-African ridges and east Pacific rise for the African and South Pacific upwellings) may diminish the plate-driving potential of upwellings. By contrast, downwellings tend to occur beneath subducting plate boundaries, and thus should tend to generate tractions beneath old oceanic or continental lithosphere, where thicker lithosphere will allow for the transmission of larger tractions. Because we use a radial viscosity structure in this work, we cannot rule out the possibility that the addition of temperature-dependent viscosity or lateral variations in lithospheric thickness will tend to diminish the plate-driving potential of upwelling flow.

It is possible that incomplete ray coverage of the mantle by tomography, particularly systematic differences between positive and negative seismic velocity anomalies, may influence our results. However, we have shown that slab densities inferred from tomography produce a good fit to plate motions, suggesting adequate resolution of slab material by the S20RTSb tomography model. We have no reason to suspect that negative velocity anomalies are more poorly resolved in this tomography model. In addition, unmodeled factors such as plate bending at subduction zones (Conrad and Hagar, 1999), normal tractions across transform faults or continental collisions (Richards and Lithgow-Bertelloni, 1996), non-Newtonian mantle vis-

cosity (Becker, 2006), variations in the slab pull force due to slab detachment (Conrad et al., 2004), and amplified plate-mantle coupling beneath continental roots (Conrad and Lithgow-Bertelloni, 2006) may affect the force balance on plates. As a result, future studies may find that one or more of these influences, when combined with upwelling flow, produces an improved fit to plate motions.

6. Conclusions

Our results suggest that active upwelling flow in the mantle does not contribute significantly to the forces that drive plate motions. Instead, we found that downwelling flow associated with slab descent (slab pull in the upper mantle and slab suction in the lower mantle (Conrad and Lithgow-Bertelloni, 2002, 2004)) is significantly more important for driving plate motions. In nearly every case, we have found that the addition of active mantle upwelling to slab-induced downwelling flow degrades the overall fit to plate motions. The one situation in which active upwelling and downwelling flow can coexist in the mantle to produce a good fit to plate motions occurs if the magnitude of mantle density heterogeneity is small enough so that the resulting flow does not overwhelm the slab pull force. This can be achieved only if the conversion factor between tomographic seismic velocity anomaly and density is at the low end of the expected range (TCF $\sim 0.05 \, \mathrm{g \, cm^{-3} \, km^{-1} \, s}$). However, this solution yields a volume of mantle slab material that is significantly smaller than the expected volume based on plate reconstructions. Thus, we favor a solution in which upwelling flow originating in the lower mantle does not act as a significant driver of plate motions.

If upwelling flow in the lower mantle is not a significant driver of plate motions, then we need to explain the dynamics of large, seismically slow anomalies in the lower mantle beneath Africa and the South Pacific. One possibility is that these regions do represent hot thermal upwellings, but that the flow induced by these upwellings is decoupled from the surface plates. This decoupling could result from low sub-lithospheric viscosities associated with the thermal anomaly or the positioning of upwellings beneath the center of plates. If this is the case, then the introduction temperature-dependent viscosity or lithospheric thickness variations may decrease the sensitivity of surface plate motions to upwelling flow. Alternatively, the absence of upwelling flow as a plate-driving force may indicate that the lower mantle negative velocity anomalies are not thermal in origin, and thus do not drive upwelling flow. In this case, the use of tomographic images to infer mantle density heterogene-

ity must be called into question, particularly for slow velocity anomalies in the lower mantle, This conclusion agrees with geodynamic and seismic evidence for chemical reservoirs of compositionally distinct "piles" of fluid in the lower mantle that are associated with lower mantle negative seismic velocity anomalies (e.g., Kellogg et al., 1999; van der Hilst and Karason, 1999; Masters et al., 2002; Ni et al., 2002) that do not participate in mantle-scale flow (e.g., Davaille, 1999; McNamara and Zhong, 2004, 2005). In this case, the tomographically imaged low velocity anomalies beneath Africa and the South Pacific do not represent active upwelling because they are dynamically passive structures associated with chemically distinct and temporally stable reservoirs in the lower mantle (e.g., van Thienen et al., 2005).

Acknowledgements

References

Becker, T.W., 2006. On the effect and strain-rate dependent viscosity on global mantle flow, net rotation, and plate driving forces. Geophys. J. Int. 168, 843–862.

Becker, T.W., Boschi, L., 2002. A comparison of tomographic and geodynamic mantle models. Geochem. Geophys. Geosyst. 3, 1003, doi:10.1029/2001GC000168.

Becker, T.W., O'Connell, R.J., 2001. Predicting plate motions with mantle circulation models. Geochem. Geophys. Geosyst. 2 (12), doi:10.1029/2001GC000171.

Becker, T.W., Kellogg, J.B., Ekstrom, G., O'Connell, R.J., 2003. Comparison of azimuthal anisotropy from surface waves and finite-strain from global mantle-circulation models. Geophys. J. Int. 155, 696–714.

Behn, M.D., Conrad, C.P., Silver, P.G., 2004. Detection of upper mantle flow associated with the African Superplume. Earth Planet. Sci. Lett. 224, 259–274.

Bird, P., 2003. An updated digital model of plate boundaries. Geochem. Geophys. Geosyst. 4, 1027, doi:10.1029/2001GG000252.

Conrad, C.P., Gurnis, M., 2003. Mantle flow, seismic tomography and the breakup of Gondwanaland: integrating mantle convection backwards in time. Geochem. Geophys. Geosyst. 4, 1031, doi:10.1029/2001GC000299.

Conrad, C.P., Hagar, B.H., 1999. The effects of plate bending and fault strength at subduction zones on plate dynamics. J. Geophys. Res. 104, 17551–17571.

Conrad, C.P., Lithgow-Bertelloni, C., 2002. How mantle slabs drive plate tectonics. Science 298, 207–209.

Conrad, C.P., Lithgow-Bertelloni, C., 2004. The temporal evolution of plate driving forces: importance of "slab suction" versus "slab pull" during the Cenozoic. J. Geophys. Res. 109, B10407, doi:10.1029/2004JB002991.

Conrad, C.P., Lithgow-Bertelloni, C., 2006. Influence of continental roots and asthenosphere on plate–mantle coupling. Geophys. Res. Lett. 33, L05312, doi:10.1029/2005GL025621.

Conrad, C.P., Bilek, S., Lithgow-Bertelloni, C., 2004. Great earthquakes and slab pull: interaction between seismic coupling and plate–slab coupling. Earth Planet. Sci. Lett. 218, 109–122.

Davaille, A., 1999. Simultaneous generation of hotspots and superswells by convection in a heterogeneous planetary mantle. Nature 402, 756–760.

Davies, G.F., 1988. Ocean bathymetry and mantle convection. 1. Large scale flow and hotspots. J. Geophys. Res. 93, 10467–10480.

DeMets, C., Gordon, R.G., Argus, D.F., Stein, S., 1994. Effect of recent revisions to the geomagnetic reversal time scale on estimates of plate motions. Geophys. Res. Lett. 21, 2191–2194.

Dziewonski, A.M., Woodhouse, J.H., 1987. Global images of the earth's interior. Science 236, 37–48.

Elsasser, W.M., 1969. Convection and stress propagation in the upper mantle. In: Runcorn, S.K. (Ed.), The Application of Modern Physics to the Earth and Planetary Interiors. Wiley-Interscience, London, pp. 223–246.

Forsyth, D., Uyeda, S., 1975. On the relative importance of the driving forces of plate motion. Geophys. J. Roy. Astron. Soc. 43, 163–200.

Gordon, R.G., Jurdy, D.M., 1986. Cenozoic global plate motions. J. Geophys. Res. 91, 12389–12406.

Grand, S.P., van der Hilst, R.D., Widiyantoro, S., 1997. Global seismic tomography: a snapshot of convection in the earth. GSA Today 7, 1–7.

Gurnis, M., Mitrovica, J.X., Ritsema, J., van Heijst, H.-J., 2002. Constraining mantle density structure using geological evidence of surface uplift rates: the case of the African superplume. Geochem. Geophys. Geosyst. 1 (7), doi:10.1029/1999GC000035.

Hagar, B.H., O'Connell, R.J., 1979. Kinematic models of large-scale mantle flow. J. Geophys. Res. 84, 1031–1048.

Hager, B.H., O'Connell, R.J., 1981. A simple global model of plate dynamics and mantle convection. J. Geophys. Res. 86, 4843–4867.

Karato, S.-I., Karki, B.B., 2001. Origin of lateral variation of seismic wave velocities and density in the deep mantle. J. Geophys. Res. 106, 21771–21783.

Kellogg, L.H., Hagar, B.H., van der Hilst, R.D., 1999. Compositional stratification in the deep mantle. Science 283, 1881–1884.

Li, X.D., Romanowicz, B., 1996. Global mantle shear velocity model developed using non-linear asymptotic coupling theory. J. Geophys. Res. 101, 22245–22272.

Lithgow-Bertelloni, C., Guynn, J.H., 2004. Origin of the lithospheric stress field. J. Geophys. Res. 109, B01408, doi:10.1029/2003JB002467.

Lithgow-Bertelloni, C., Richards, M.A., 1998. The dynamics of Cenozoic and Mesozoic plate motions. Rev. Geophys. 36, 27–78.

Lithgow-Bertelloni, C., Silver, P.G. S, 1996. Dynamic topography and driving torques due to lower mantle upwellings. In: American Geophysical Union Fall Meeting, San Francisco, CA, T32D-06.

Lithgow-Bertelloni, C., Silver, P.G., 1998. Dynamic topography, plate driving forces and the African superswell. Nature 395, 269–272.

Masters, G., Laske, G., Bolton, H., Dziewonski, A., 2002. The relative behavior of shear velocity, bulk sound speed, and compressional velocity in the mantle: implications for chemical and thermal structure, in earth's deep interior: mineral physics and tomography from the atomic to the global scale. In: Karato, S., et al. (Eds.), Geophys. Monogr. Ser., vol. 117. AGU, Washington, DC, pp. 63–87.

McNamara, A.K., Zhong, S., 2004. Thermochemical structures within a spherical mantle: superplumes or piles? J. Geophys. Res. 109, B07402, doi:10.1029/2003JB002847.

McNamara, A.K., Zhong, S., 2005. Thermochemical structures beneath Africa and the Pacific Ocean. Nature 437, 1136–1139.

Ni, S., Tan, E., Gurnis, M., Helmberger, D., 2002. Sharp sides to the African superplume. Science 296, 1850–1852.

O'Connor, J.M., Le Roex, A.P., 1992. South Atlantic hotspot-plume systems. 1. Distribution of vulcanism in time and space. Earth Planet. Sci. Lett. 113, 343–364.

Ricard, Y., Richards, M.A., Lithgow-Bertelloni, C., Le Stunff, Y., 1993. A geodynamic model of mantle density heterogeneity. J. Geophys. Res. 98, 21895–21909.

Richards, M.A., Lithgow-Bertelloni, C., 1996. Plate motion changes, the Hawaiian-Emperor bend, and the apparent success and failure of geodynamics models. Earth Planet. Sci. Lett. 137, 19–27.

Richards, M.A., Duncan, R.A., Courtillot, V.E., 1989. Flood basalts and hot-spot tracks: plume heads and tails. Science 246, 103–107.

Richter, F., McKenzie, D., 1978. Simple plate models of mantle convection. J. Geophys. 44, 441–471.

Ritsema, J., van Heijst, H.J., Woodhouse, J.H., 1999. Complex shear wave velocity structure related to mantle upwellings beneath Africa and Iceland. Science 286, 1925–1928.

Ritsema, J., van Heijst, H.J., Woodhouse, J.H., 2004. Global transition zone tomography. J. Geophys. Res. 109, B02302, doi:10.1029/2003JB002610.

Steinberger, B., 2000. Slabs in the lower mantle: results of dynamic modeling compared with tomographic images and the geoid. Phys. Earth Planet. Int. 118, 241–257.

Steinberger, B., Schmeling, H., Marquart, G., 2001. Large-scale lithospheric stress field and topography induced by global mantle circulation. Earth Planet. Sci. Lett. 186, 75–91.

Su, W., Woodward, R.L., Dziewonski, A.M., 1994. Degree 12 model of shear velocity heterogeneity in the mantle. J. Geophys. Res. 99, 6945–6981.

Thoraval, C., Richards, M.A., 1997. The geoid constraint in global geodynamics: viscosity structure, mantle heterogeneity models and boundary conditions. Geophys. J. Int. 131, 1–8.

Turcotte, D.L., Oxburgh, E.R., 1967. Finite amplitude convective cell and continental drift. J. Fluid Mech. 28, 29–42.

van der Hilst, R.D., Karason, H., 1999. Compositional heterogeneity in the bottom 1000 kilometers of Earth's mantle: toward a hybrid convection model. Science 283, 1885–1888.

van der Hilst, R.D., Widiyantoro, S., Engdahl, E.R., 1997. Evidence for deep mantle circulation from global tomography. Nature 386, 578–584.

van Thienen, P., van Summeren, J., van der Hilst, R.D., van den Berg, A.P., Vlaar, N.J., 2005. Possible early origin and long term stability of deep chemically distinct mantle reservoirs. Geophysical Monograph, vol. 160. American Geophysical Union, Washington, DC, pp. 117–136.